



# Effects of Primary Welding Parameters on FCAW Steel Weld Form

Memduh Kurtulmuş<sup>1\*</sup>

<sup>1</sup> Marmara University, School of Applied Science, 34722 Goztepe/Istanbul

(First received 05 April 2018 and in final form 27 April 2018)

## Abstract

Flux Cored Arc Welding (FCAW) has been a viable welding process for structural steel erection, heavy equipment repair, bridge construction and other similar applications. The primary welding parameters (welding current, welding speed and arc voltage) determine FCAW weld geometry, weld mechanical properties and weld quality. In this study bead on plate welds were produced on SAE 1015 steel work pieces. Metallographic investigations were done on the cross-sectional of the welds. The effects of the primary welding parameters on weld components (penetration depth, reinforcement height, width, reinforcement contact angle, reinforcement area and penetration area) were measured. The effects of primary welding parameters on weld bead geometry are presented in graphical forms.

**Keywords:** Flux cored arc welding; arc welding parameters; weld bead geometry; weld geometry components.

## Birincil Kaynak Parametrelerinin FCAW Çelik Kaynak Formuna Etkileri

### Öz

Öznlü tel ark kaynağı yüksek ergime gücü ve yüksek kaliteli dikiş üretme özelliğine sahip olduğundan kullanımı sürekli artmaktadır. Bu özelliklerin korunması için öznlü tel ark kaynağı parametrelerinin yakından kontrol edilmesi gerekmektedir. Kaynak akımı ve kaynak geriliminin etkisini ortaya çıkarmak için alaşımız çelik levhalar üzerine öznlü tel ark kaynak yöntemi ile kör dikişler çekilmiştir. Dikişlerin genişlik, nüfuziyet ve taşıma yükseklikleri, eriyen ve yığılan metal kesit alanları ile dikiş yüzeyi açıları ölçülmüştür. Her kaynak parametresinin dikiş geometri boyutları üzerindeki tesirini ortaya çıkaran grafikler çizilmiştir.

**Anahtar kelimeler:** Akı öznlü ark kaynağı; ark kaynağı parametreleri; kaynak boncuk geometrisi; kaynak geometrisi bileşenleri

## 1. Introduction

Flux cored arc welding (FCAW) uses a wire that contains materials in its core that, when burned by the heat of the arc, produces shielding gases and fluxing agents to help produce a sound weld without the need for external shielding gas. The shielding can endure a strong breeze. When finished, the weld is covered with slag that must be removed [1]. FCAW is a variant of the MIG/MAG process. The only difference lies in the electrode. The FCAW electrode is a tubular wire which contains flux in it. During the welding operation, the flux of electrode melts and produces a shielding gas and a liquid flux. The arc area is covered by the shielding gas. The weld pool is protected from the atmosphere by the gas and the slag. The welding pool can also be protected by extra shielding gases. Mostly carbon dioxide is used. FCAW may be applied semi automatically or automatically.

The semiautomatic FCAW process is a highly productive process for structural steel fabrication [2] and repair [3-5]. FCAW

is also popular in weld cladding [6,7]. The FCAW process offers distinct advantages over the welding processes which makes it highly popular [2]. It also has cost advantages. The advantages of FCAW are summarized below:

- It has a precise control on welding current and welding energy,
- High metal deposition rates,
- More tolerance to rust and mill scale,
- Low spatters and low cost for shielding gas,
- Less operator skill required,
- Suitable for robotic welding and
- High weld quality.

<sup>1</sup> Corresponding Author: Marmara University, School of Applied Science, 34722 Goztepe/Istanbul, [memduhk@marmara.edu.tr](mailto:memduhk@marmara.edu.tr)

The profile of a weld bead has been determined to have a significant influence on welding quality [8]. A weld bead geometry and its components are schematically defined in Figure 1[9]. The primary welding parameters (welding current, arc voltage and welding speed) directly controls the welding energy and determines the size of each weld bead geometry component [1,10]. Generally the volume of the weld increases with the welding energy. The welding energy is calculated from equation 1 [11].

$$H = \frac{I.E.f}{S} \quad (1)$$

- I : Welding current
- E : Arc voltage
- S : Welding speed
- f : Arc efficiency

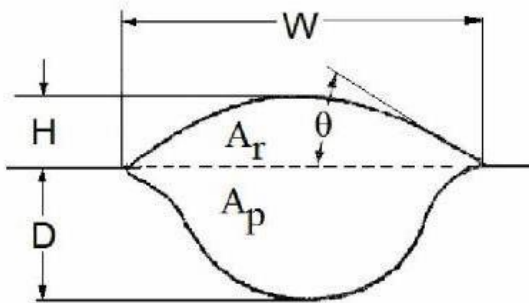


Figure 1. The cross-sectional appearance of a bead on plate weld and the weld components [9]. Ar: Reinforcement area, Ap: Penetration area, D: Penetration depth, H: Reinforcement height, W: Bead width,  $\theta$ : Reinforcement contact angle.

The cross-sectional area of the weld bead controls the cooling rate of the weldment [11]. Thus, the weld cross-sectional area determines the mechanical properties of the weld metal [12]. The fatigue properties of a weld is indirectly proportional with the reinforcement contact angle of the weld [9] The weld width (W) [12] and the ratio of penetration depth to weld width (D/W) [9] has a direct effect on weld pool shrinkage and shrinkage stresses respectively. The welding stresses and the cracking tendency of the weld increases with W and D/W ratio. The mechanical properties and cracking risk of a weld are directly dependent upon the volume [13] and form of the weld cross-sectional area [14].

The importance of primary welding parameters on weld geometry, mechanical properties and weld quality is clearly explained in the above paragraph. Optimal selection of these welding parameters is required for the high quality joining and also for cost effectiveness [1]. Therefore, optimal welding parameters have to chosen for desired joining operations [15]. Various optimization methods, such as, Taguchi method [16, 17], fractional factorial technique [18], linear regression [19], response surface methodology [20] and artificial neural networks [21] have been applied to various welding processes. Several optimization papers for the FCAW process have been published [22-28]. In these papers, the effects of welding current, welding speed, arc voltage and nozzle to plate distance were experimentally investigated.

In FCAW, primary welding parameters directly control the heat of the arc [30], and determine the weld geometry and mechanical properties. This study is intended to fully explain the effects of FCAW welding current, arc voltage and welding speed on the size of FCAW weld components.

## 2. Experimental

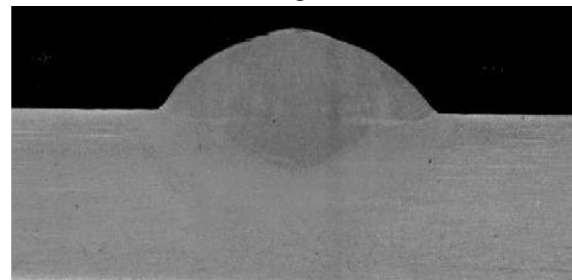
In the experimental procedure of this study a 10 mm thick SAE 1015 steel plate was used. The chemical properties of the plate is presented in Table 1. 350x100 mm welding test pieces were obtained from the plate by the laser cutting process. In cutting operation the longitudinal direction of the piece was chosen parallel to the rolling direction of the plate.

Bead on plate welds were produced with a semi automatic Askaynak Magtronik 500 W FCAW welding machine. Prior to the welding operations, the surface of work pieces were cleaned with an abrasive wheel and asetone. The welding torch was kept at an inclination of 85° to the pull direction. The speed of the torch was electronically controlled..

1.2 mm diameter AWS E71T-C rutile filler wire was consumed in welding. A 19.5 mm distance between the work piece and the contact tip was kept constant in welding applications. No preheating was done. CO2 shielding gas flow was kept at 12 lt/min in every welding. Only 300 mm long weld was produced on each work piece. After finishing the welding processes, the welds were cut perpendicular to the welding direction by using a power hacksaw. A 25 mm long piece from the beginning and the rear of the weld were cut out. The remaining of the weld was cut into 5 equal specimens. The cut surfaces of the specimens were polished with abrasive papers. Then the specimens were etched using 8% nital solution to reveal the weld bead size and shape. The etched sections were scanned to 1000% of the original size in a scanner and each weld bead was photographed. The weld bead geometry parameters were measured by using a planimeter, a ruler and a protractor on a macrostructure image photograph. We obtained 5 different results for each welding condition. Arithmetic average of the results were calculated to determine the weld bead geometry parameter.

## 3. Results and Discussion

Figure 2 shows a typical macroscopic cross section of a weld bead. Measurements were done on peach photograph. Then mathematical averages were calculated. The obtained experimental results were presented by series of graphics. The results were discussed according to the effects of each welding



parameter.

Figure 2. Typical macrograph of a weld bead.

### 3.1. Effects of Welding Current

In welding current effect tests, 26.5 volts arc voltage and 4.5 mm/s welding speed were kept constant in welding operations. In welding operations, the welding current was varied between 190-310 Amperes. Figure 3 shows the effects of welding current on the weld bead components. The increase in the welding current caused a higher welding input energy according to the Equation 1 [29]. More energy was produced with a high current which resulted in a bigger weld size. Thus, the total weld bead cross-section area ( $A_t$ ) was found to be enlarged with the welding current.  $A_t$  is obtained by adding the reinforcement area ( $A_r$ ) to the penetration area ( $A_p$ ) [9], where  $A_t$  is the indicator of the weld bead size. The total weld bead area gets larger linearly with increase in welding current as indicated in Figure 3a. Figure 3b shows the weld bead cross-section area growth trend with the welding current.  $A_r$  and  $A_p$  increase linearly with the welding current, but the slope of each line is different. The growth rate of the  $A_r$  is bigger than the growth rate of the  $A_p$ . The size of  $A_r$  and  $A_p$  are roughly identical at 190 Amperes welding current. The size difference between them significantly appears with the welding current [31]. When the passing current increases the current density in the electrode also increases [32]. A higher welding current density causes more heating of the electrode and hence larger volume of the electrode melts [33]. The droplet formation frequency and droplet temperature increase with the current density [9]. The welding current also increases the falling velocity of a droplet [9]. The weld pool size gets larger with the welding current due to the high electrode melting rate [34]. The growth of the weld pool size results in an important increase in  $A_r$  as shown in Figure 3b. With the pool size the heat being transferred to the base metal from the weld pool increases. More melting of the base metal occurs by high energy transfer and this leads to a rise in  $A_p$ . However, the increase in  $A_p$  is not as big as the increase of  $A_r$ . High energy formation with the welding current enlarges the weld width as shown in Figure 3c. The enlargement of the  $A_p$  causes an increase in the weld width. The growth rate of the weld width is proportional to the growth rate of the  $A_p$ . The increase of the welding current results in a remarkable increase in the penetration depth as shown in Figure 3d. The increase in heat put transfer and the momentum of liquid electrode droplets induce a deeper penetration of the weld pool [9]. The growth rate of the penetration depth is bigger than the penetration area growth rate. The welding current has a considerable effect on the reinforcement height. Figure 3e indicates that the reinforcement height increases with the welding current. The high increase in  $A_r$  causes a major increase in the reinforcement height. The ascending welding current produces an increase in the reinforcement height and hence an important growth in the reinforcement contact angle as shown in Figure 3f.

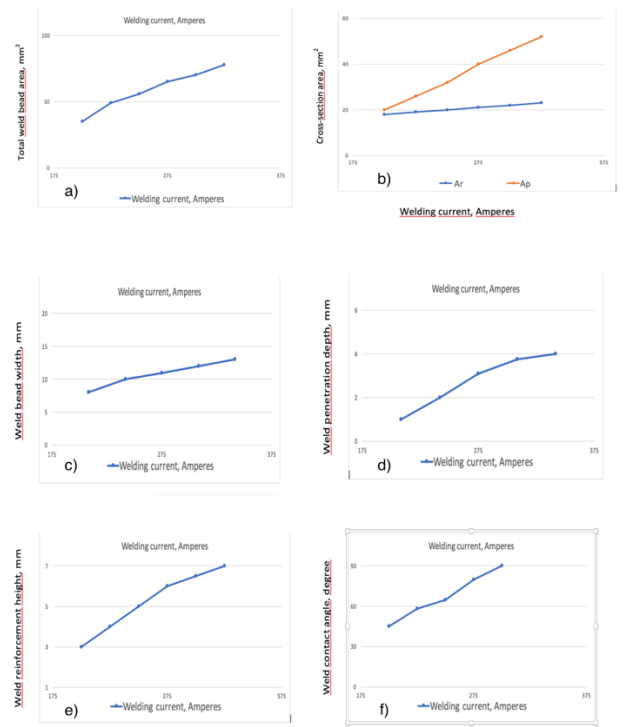


Figure 3. Effects of welding current on weld components. parameters: (a) Weld bead size, (b) Weld reinforcement and penetration area, (c) Weld bead width, (d) Weld penetration depth, (e) Weld reinforcement height and (f) Weld reinforcement contact angle.

### 3.2. Effects of Arc Voltage

In arc voltage effect tests 220 Amperes welding current and 4.5 mm/s welding speed were kept constant in welding operations. In welding operations, the arc voltage was varied between 26.5-32.5 volts. The welding input energy increases with the arc voltage according to the Equation 1. Figure 4 shows the effects of arc voltage on weld bead geometry. The Figure 4a illustrates that the total weld bead cross-section area increases linearly with the arc voltage. The slope of this line is smaller than the slope of Figure 3a's. The comparison of the lines illustrates that the arc voltage has a less effect on the weld bead size than the welding current. The increase in the heat input with the arc voltage makes a negligible effect on the electrode melting rate [10]. There is a small increase in the melted electrode volume with the arc voltage [27]. Thus, small increases in  $A_p$  and  $A_r$  occurred with the increasing arc voltage as shown in Figure 4b. Figure 4a shows that small amounts of growth in  $A_p$  and  $A_r$  result in a small growth in the weld bead size (Figure 4a). In electric arc welding operations the arc forms between the base metal and the electrode. The increase of the arc voltage enlarges the bottom part of the arc [1]. Thus, more heating and thus more melting occurs on the surface of the base metal. This wide melting produces a wide weld pool [35,36]. The effect of the arc voltage on the weld width is shown in Figure 4c. The weld width shows a big increase with arc voltage because of wide weld pool formation [7,34]. The comparison of Figure 4c and 3c shows that arc voltage is more effective on the weld width than the welding current. Figure 4d shows that the arc voltage causes a small increase in penetration depth. The heat input gain with the arc voltage was mainly consumed on widening of the weld bead. As a result, a small increase in penetration depth occurred.

Figure 4e shows that the reinforcement height decreases with arc voltage. A small increase in weld bead size and a big growth

of the weld width are obtained with increasing the arc voltage. These changes cause the decrease of the reinforcement height. The decrease of the reinforcement height and increase of the weld width jointly cause the decrease of the reinforcement contact angle as shown in Figure 4f. Similar results were obtained in GMAW [37] and other FCAW operations [38- 40].

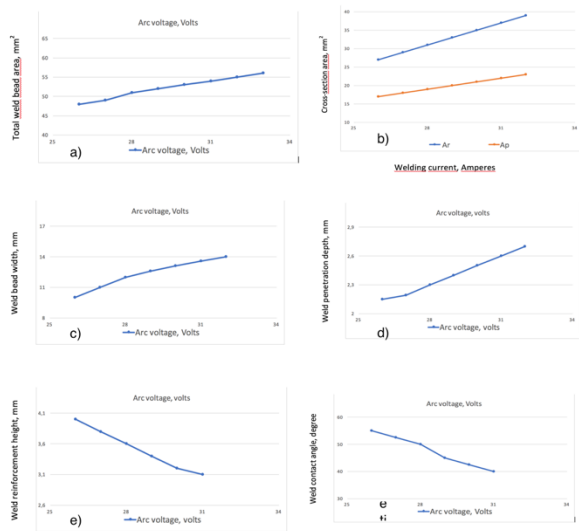


Figure 4. Effects of arc voltage on weld bead components: (a) Weld bead size, (b) Weld reinforcement and penetration area, (c) Weld bead width, (d) Weld penetration depth, (e) Weld reinforcement height and (f) Weld reinforcement contact angle.

### 3.3. Effects of Welding Speed

In welding speed effect tests, 300 Amperes welding current and 32 volts arc voltage were kept constant in the welding operations. In the welding operations, the welding speed was varied between 3.7-5.3 mm/s. Equation 1 shows that the welding input energy reduces with the welding speed. This reduction in the welding heat input lowers the melting rate of the electrode and less base metal is heated. The combined effects of less heating and small energy input resulted a decrease in metal deposition rate and base metal melting rate. The effects of the welding speed on weld bead components are indicated in Figure 5. Figure 5a shows that the welding speed cause a decrease in the weld bead size. Figure 5b shows that weld metal deposition and base metal melting are reduced with the welding speed. These reductions are the reasons of the small weld bead size. The small weld bead size causes a narrow weld bead (Figure 5c), a small penetration depth (Figure 5d), a small reinforcement height (Figure 5e) and a small reinforcement contact angle (Figure 5f).

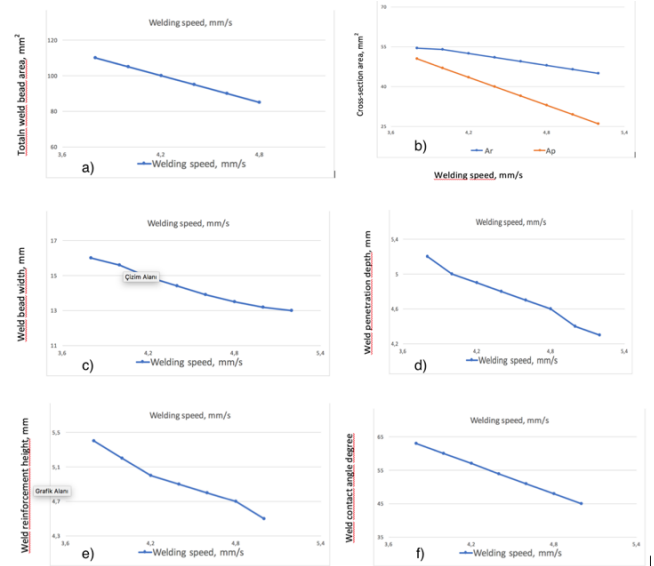


Figure 5. Effects of welding speed on weld bead components: (a) Weld bead size, (b) Weld reinforcement and penetration area, (c) Weld bead width, (d) Weld penetration depth, (e) Weld reinforcement height and (f) Weld reinforcement contact angle.

## 4. Conclusions and recommendations

The measurements done on FCAW bead on plate weld photographs lead to the following conclusions.

1. An increase in the welding speed causes a decrease in every property of the weld component.
2. An increase in the welding current causes an increase in the weld bead size, weld width, penetration depth, reinforcement height and reinforcement contact angle.
3. The arc voltage increases the weld width, the weld size and a slight penetration depth.
4. The reinforcement height and the reinforcement contact angle decrease with an increase in the arc voltage.

## References

- [1] Carry, H.B., Helzer, S.C., 2005. Modern Welding Technology, Prentice Hall, New York.
- [2] Blognnett, O.W., Funderburk, R.S., Miller, D.K., Quintana, M., 1999. Arc Welding Foundation, Cleveland.
- [3] Mitchell, K.C., 2003. Operation Maintenance and Materials 2, 1.
- [4] Aloraier, A., Al-Mazrouee, A., Price, J.W.H., Shetata, T., 2010. Inter. J. Press. Vessels. Piping., 87, 127.
- [5] Aloraier, A., Ibrahim, R., Thomson, P., 2006. Inter. J. Press. Vessels. Piping., 83, 394.
- [6] Palani, P.K., Murugan, N., Karthiyekan, B., 2006. Mater. Sci. Technol., 22, 1193.
- [7] Palani, P.K., Murugan, N., 2007. J. Mater. Proces. Technol., 190, 291.
- [8] Pal, S., Pal, S.K., Samantaray, A.K., 2008. J. Mater. Proces. Technol., 202, 464.
- [9] Yukler, I., Calis I., 1999. MUTEF Publications., Istanbul.
- [10] Murugan, N., Gunaraj, V., 2005. J. Mater.

- Proces. Technol., 168, 478.
- [11]Kou, S., 1987. *Welding Metallurgy*, John Wiley and Sons, New York.
- [12]Dey, V., Pratihari, D.K., Datta, G.L., Jha, M.N., Saha, T.K., Bapat, A.V., 2009. *J. Mater. Proces. Technol.*, 209, 1151.
- [13]Sandor, T., Dobranszky, J., 2007. *Mater. Sci. Forum.*, 63, 537.
- [14]Bauber, B., Topia, Kralj, S., Kouh, Z., 2011. *Mater. Technol.*, 45, 413.
- [15]De, A., Jantre, J., Ghosh, P.K., 2004. *Sci. Technol. Weld. Join.*, 9, 253.
- [16]Benyounis, K.Y., Olabi, A.G., 2008. *Adv. Eng. Software.*, 39, 483.
- [17]Eeme, U., Bayramoglu, M., Kazancuoglu, Y., Ozgun, S., 2009. *Mater. Technol.*, 43, 143.
- [18]Bilici, M.K., Yukler, A.I., Kurtulmus, M., 2011. *Mater. Des.*, 32, 4074.
- [19]Murugan, N., Parmar, R.S., 1994. *J. Mater. Proces. Technol.* 41, 381.
- [20]Kim, I.S., Son, K.J., Yang, Y.S., Yaragada, P.K.D.V., 2003. *J. Mach. Tool. Manuf.*, 43, 763.
- [21]Koleva, E., Vuchkov I., 2005. *Vacuum*, J., 77, 423.
- [22]Okuyucu, H., Kurt, A., Arcakoglu, E., 2007. *Mater. Des.*, 29, 78.
- [23]Raveendra, J., Parmar, R.S., 1987. *J. Metal. Cons.*, 19, 31.
- [24]Sudhakaran, R., Vel-murugan, V., Sivasakthinal, P.S., 2012. *J. Eng. Research.*, 9, 64.
- [25]Rodrigues, L.O., Paiva, A.P., Costa, S.C., 2009. *Welding. Inter.*, 23, 261.
- [26]Starling, C.M.D., Modenesi, P.J., Borba, T.M.D., 2010. *Welding. Inter.* 24, 485.
- [27]Kanman, T., Murugan, N., 2006. *J. Mater. Proces. Technol.* 176, 230.
- [28]Palani, P.K., Murugan, N., 2006. *Inter. J. Advan. Manuf. Technol.*, 30, 669.
- [29]Sadek, A., Ibrahim, R.N., Price, J.W.H., Shetata, T., Ushio, M., 2001. *Trans. Japan. Welding. Research. Ins.*, 30, 45.
- [30]Rajkumar, G.B., Murugan, N., 2012. *J. Sci. Research.*, 78, 85.
- [31]Gomes, J.H.F., Costa, S.C., Paiva, A.P., Balestrassi, P.P., 2012. *J. Mater. Eng. Perform.*, 21, 918.
- [32]Singh, R.P., Garg, R.K., Shukla, D.K., 2012. *Inter. J. Eng. Sci. Technol.*, 4, 747.
- [33]Srivastava, B.K., Tewari, S.P., Prakasha, J., 2010. *Inter. J. Eng. Sci. Technol.*, 2, 1425.
- [34]Gunaraj, V., Murugan, N., 1999. *J. Mater. Proces. Technol.*, 88, 266.
- [35]Alam, S., Khan, M.I., 2011. *Inter. J. Eng. Sci. Technol.*, 3, 7408.
- [36]Hrabe, P., Choteborsky R., Navratilova, M., 2009. *Inter. Conf. Eco. Eng. Manuf. Systems, Brasov, 26-27 November, Romanya.*
- [37]Kolahan, F., Heidari, M., 2011. *J. Aerospace. Mech. Eng.*, 5, 138.
- [38]Rajkumar, C.B., Murugan, N., 2010. *Euro. J. Sci. Research.*, 78, 85.
- [39]Kumar, V.V., Murugan, N., 2011. *J. Mineral. Mater. Charac. Eng.*, 10, 827.
- [40]Nouri, M., Abdollahzadehy, A., Malek, F., 2007. *J. Mater. Sci. Technol.*, 23, 817.